Available online at www.sciencedirect.com
ScienceDirect
Nuclear Instruments and Methods in Physics Research B 252 (2006) 205–211
NIM B
Beam Interactions with Materials & Atoms
www.elsevier.com/locate/nimb

A study of oscillations in the angular distribution of volume reflected ions from bent crystals

M.B.H. Breese *

Centre for Ion Beam Applications, 2 Science Drive 3, Department of Physics, National University of Singapore, Singapore 117542, Singapore

Received 31 July 2006; received in revised form 12 September 2006
Available online 30 October 2006

Abstract

Periodic oscillations in the angular distribution of volume reflected MeV protons which are transmitted through thin, curved crystals are observed in simulations. Such periodic oscillations are present even when the lattice radius of curvature is less than the critical radius. Previous studies have predicted and observed only uniform volume reflection along the lattice curvature, and the conditions under which uniform or periodic reflection occurs are studied. Oscillations are also observed in the simulated nuclear encounter probability under similar conditions, and a similar origin is attributed. The observations are extended to higher energies to predict when similar oscillations in the volume reflected angular distribution and nuclear encounter probability may be present in present beam extraction and collimation experiments at GeV and TeV energies.

PACS: 61.85.+p; 29.27.−a; 41.75.+a

Keywords: Bent crystals; Volume reflection; Nuclear encounter probability

1. Introduction

Channeling in bent crystals has been successfully used for many years as a means of deflecting, extracting and collimating charged particle beams in high-energy accelerators [1–9]. If the lattice curvature radius is greater than a critical radius, R_c, many ions incident on the entrance face within the channeling critical angle, θ_c, are steered through the full curvature angle, δ, of the lattice and emerge aligned with the exit face. Some initially channeled ions are dechanneled at some depth within the crystal (Feeding Out). Ions incident at other tilt angles are scattered into the bent channels and steered through the remaining lattice curvature, called Feeding In or Volume Capture [2,10].

Volume Reflection [11] occurs when the incident beam becomes tangential to the curved lattice within the bulk of the crystal, rather than at the entrance face, resulting in reflection off the coherent field of curved lattice planes towards alignment with the entrance face. In recent experiments [8,12] a uniform reduction of the nuclear interaction rate was observed, extending over the full range of incident tilt angles subtended by the lattice curvature and attributed either to volume reflection or volume capture. Simulated exit angular distributions [12] for 100 GeV/u gold ions and 980 GeV protons exhibited uniform volume reflection which was independent of tilt angle. The volume reflected angular distributions were broader than for random incidence, resulting in significantly increased particle loss from the accelerator. Possibilities of beam collimation schemes based on volume reflection rather than bent crystal channeling were considered.

This paper presents detailed computer simulations of the exit angular distribution caused by volume reflection using the Monte Carlo code FLUX [13,14]. This uses a binary collision model in conjunction with the Ziegler–Biersack–Littmark potential [15] to calculate ion trajectories through

* Tel.: +65 6516 2624; fax: +65 6777 6126.
E-mail address: phymbhb@nus.edu.sg

0168-583X/$ - see front matter © 2006 Elsevier B.V. All rights reserved.
doi:10.1016/j.nimb.2006.09.011

a curved lattice. Individual collisions between an ion and a lattice atom are considered, and no use is made of a continuum planar potential so channeling effects are not assumed *a priori*, but show up as a result of the simulation of many small angle collisions. Simulations were performed at MeV proton energies where the required bending layers are thin, so simulations faster and more detailed. The conclusions are extended to higher energies to examine under what circumstances similar oscillations may be observed in current GeV and TeV beam collimation experiments.

2. Simulations of volume reflection

The trajectories of ten thousand 5 MeV protons were simulated through a curved silicon (1 1 0) lattice ($\theta_c = 0.10°$, $R_c = 16$ μm) as a function of incident tilt angle θ to the entrance planes at the crystal surface. The lattice is curved towards the $-\theta$ direction, with the exit face aligned at $\theta = -\delta$. Fig. 1 shows maps of the exit angular distribution on the horizontal axis for a range of incident tilt angles θ on the vertical axis. Here the layer is 1760 nm thick with $R = 50$ μm, giving a curvature angle of $\delta = 2.0°$. The incident beam is simulated over a wide range of tilts in increments of 0.01° ($\ll\theta_c$) and the exit angular distributions sorted in steps of 0.01°. In Fig. 1(a) the exit angles are plotted with respect to the incident beam axis, so an undeflected ion exits at 0.0° on the horizontal axis for all incident tilt angles. In Fig. 1(b) absolute exit angles are plotted, so an ion entering at $\theta = -1.0°$ exits at $-1.0°$ on the horizontal axis if it is not deflected.

When the incident beam is tilted to within $\pm\theta_c$ of alignment with the entrance face it undergoes bent crystal channeling. Ions are deflected to the left by $-\delta$ on the horizontal axis, within the white circle labeled BC in Fig. 1. Feeding out of initially channeled ions produces the horizontal region labeled FO. Feeding in (volume capture) is manifested as a diagonal region, labeled FI, to the left of the incident beam where ions are partially steered through the lattice curvature to a negative exit angle. Volume reflection is manifested as a beam portion (within the white rectangle, labeled VR) which is reflected to the right of the incident beam by positive angles up to $+\theta_c$, within the range of tilt angles from about $-\theta_c$ to $-(\delta + \theta_c)$.

It is noteworthy that the distribution in Fig. 1(b) is perfectly symmetric about the white dashed line. This is in agreement with Lindhard's rule of reversibility [16] which states that "the probability of channeled ion being scattered from a certain channeled state to a certain unchanneled state equals the probability for the opposite process" [2]. The symmetry of the feeding in and feeding out regions in Fig. 1(b) are in agreement with this. Though not considered further here, simulations up to energies of 10 GeV, in thin and thick layers, always produce angular distributions which are always symmetric with features similar to Fig. 1(b).

The thick bending layer used in Fig. 1 best highlights low intensity processes such as feeding in and feeding out and to demonstrate agreement with the reversibility rule in Fig. 1(b). This paper studies oscillations in the volume reflected beam fraction in thin layers, which are best studied by plotting the beam exit distribution with respect to the incident beam axis, in the same manner as Fig. 1(a). Fig. 2 shows maps of the exit angular distributions for different thickness bending layers and lattice curvature radii. Fig. 3(a)–(d) shows plots of the exit angular distributions corresponding to the same conditions as Fig. 2(a)–(d). Fig. 2 gives an overview of all beam interactions with the curved lattice at different incident tilt angles, whereas Fig. 3 allows for their quantitative interpretation.

A previously unreported feature of volume reflection is exhibited in the thin (220 nm) curved layers in Figs. 2 and 3(a) and (b) where the random $\theta_{rms} = 0.07°$ ($<\theta_c$). For negative tilt angles along the lattice curvature, widely differing exit angular distributions are produced, with the exit beam non-uniform in reflected angle and intensity. At periodic negative tilts there is a peak reflected up to $+\theta_c$ with a width similar to that for random incidence. At other periodic negative tilts the exit beam contains a

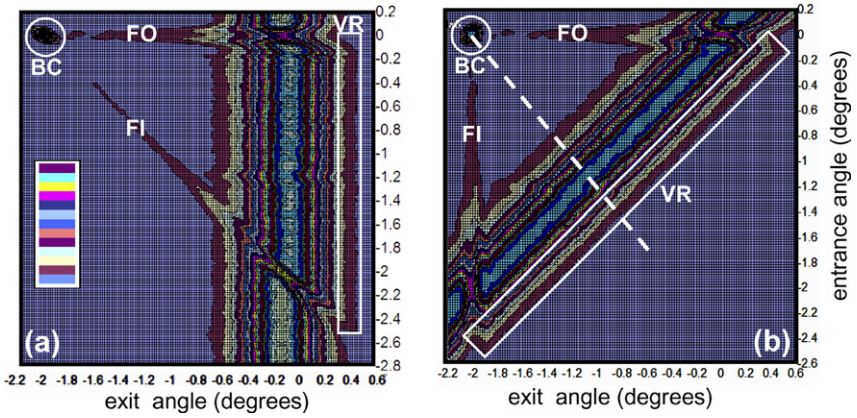

Fig. 1. Maps of the exit angular distribution on the horizontal axis for a range of incident tilt angles θ on the vertical axis. The horizontal × vertical angular dimensions are 2.8° × 2.8°. The colour scale for the exit angular intensities in increments of 5% for both maps is shown in (a), with the bottom colour corresponding to the lowest intensity. The layer thickness, curvature radius and angle are $z = 1760$ nm, $R = 50$ μm, $\delta = 2.00°$.

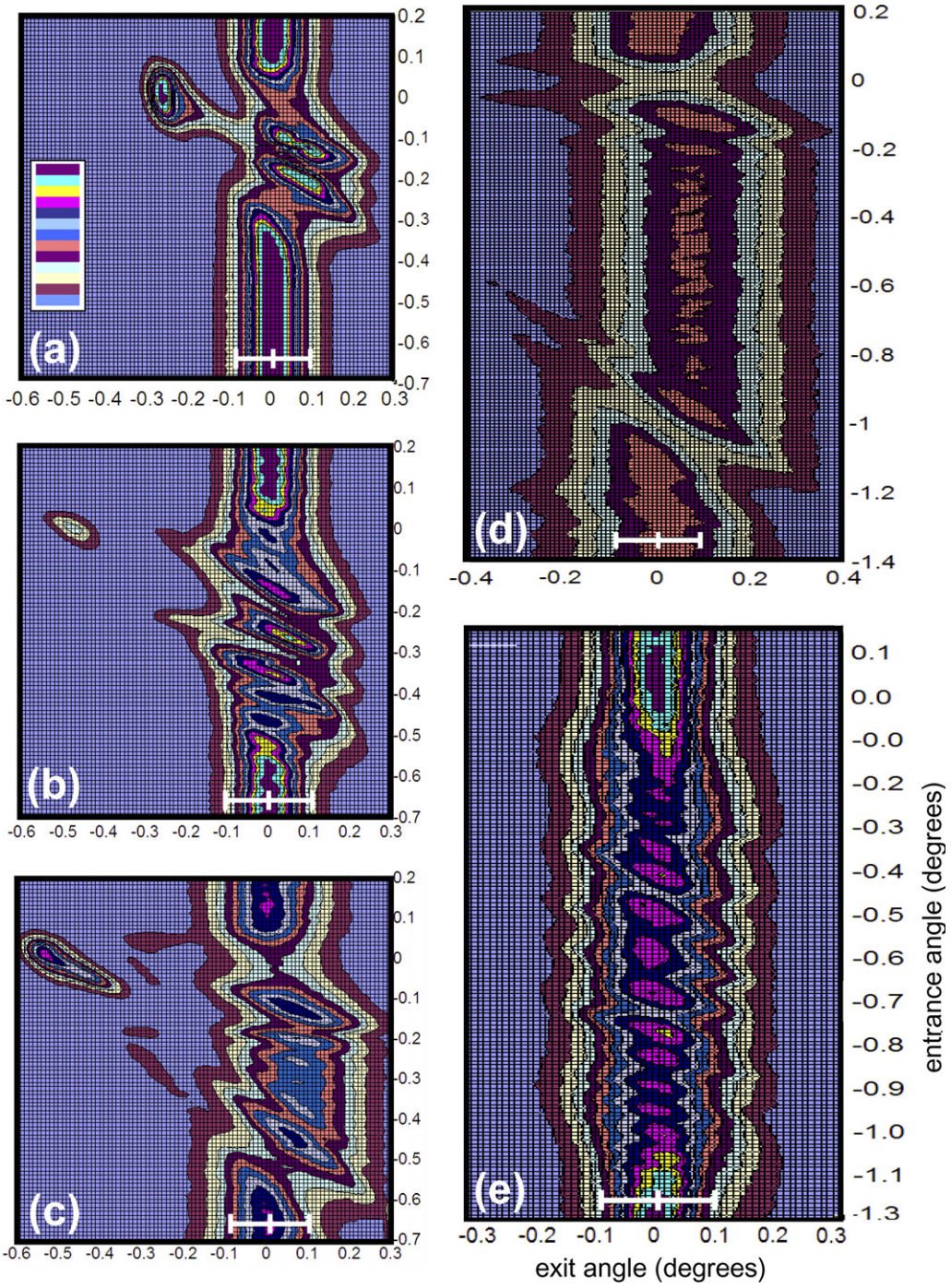

Fig. 2. Maps of the exit angular distribution on the horizontal axis for a range of incident tilt angles θ on the vertical axis. The horizontal × vertical angular dimensions are: (a), (b), (c) 0.9° × 0.9°, (d) 0.8° × 1.6°, (e) 0.8° × 1.5°. The colour scale is the same as in Fig. 1 except each colour corresponds to increments of 10%. The horizontal scale bar in each map is of length $2\theta_c = 0.20°$. The layer thickness, curvature radius and angle in each case are: (a) $z = 220$ nm, $R = 50$ μm, $\delta = 0.25°$, (b) $z = 220$ nm, $R = 25$ μm, $\delta = 0.50°$, (c) $z = 440$ nm, $R = 50$ μm, $\delta = 0.50°$, (d) $z = 880$ nm, $R = 50$ μm, $\delta = 1.00°$, (e) $z = 220$ nm, $R = 10$ μm, $\delta = 1.25°$.

smaller peak which is reflected through a smaller angle or even no peak at all.

Observation of such narrow reflected peaks in Fig. 3(a) and (b) demonstrates that there is nothing intrinsic to volume reflection which results in a wide exit angular distribution. There is a beam portion which does not undergo volume reflection, or is reflected through a smaller angle so the exit angular distribution typically contains two or even three peaks separated by θ_c. It is this range of possible exit angles which produces such a wide volume reflected angular distribution, which extends at least θ_c beyond that for random incidence. Along the lattice curvature the volume reflected distributions are of width $\theta_{rms} = 0.12°$–0.14°, up to twice that for random incidence. Such periodic

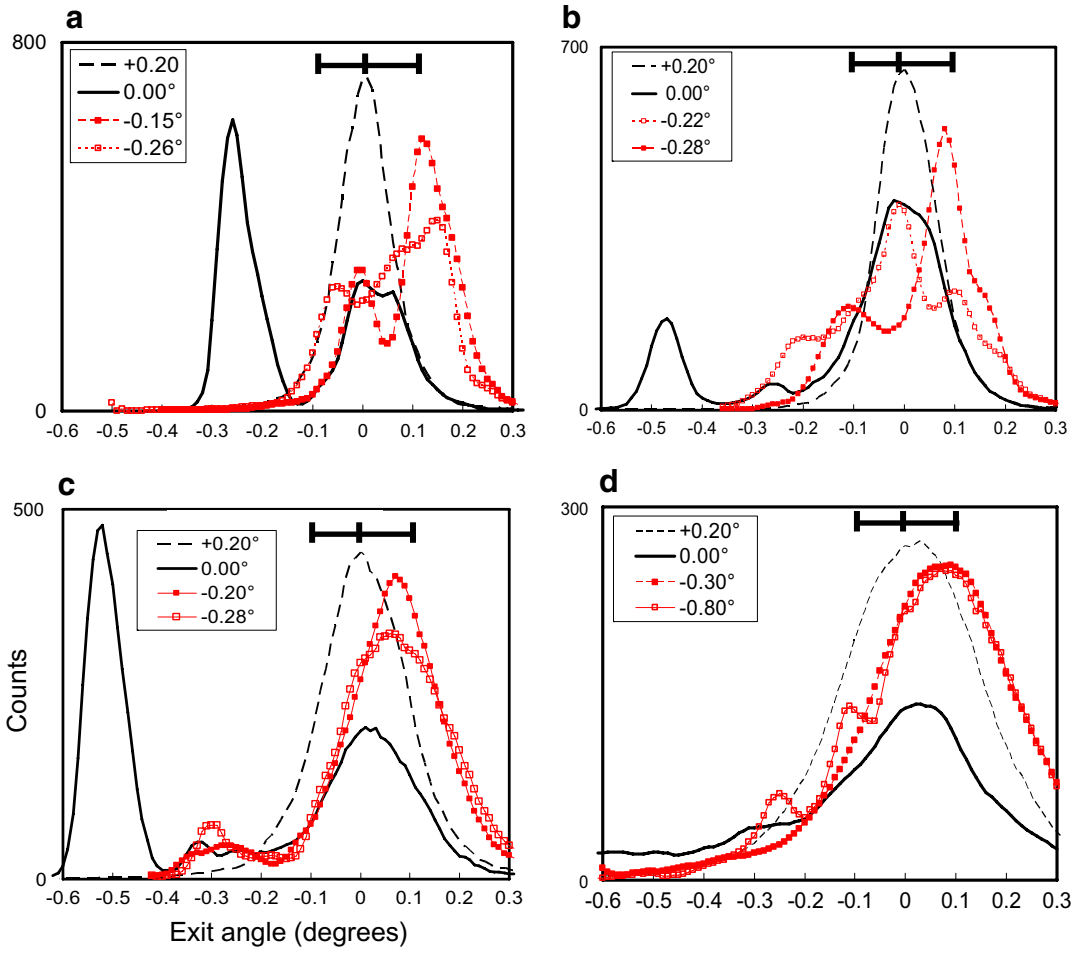

Fig. 3. Exit angular distributions corresponding to the maps in Fig. 2(a–d). Exit angular distributions for random incidence at $\theta = +0.20°$ (dashed black line) and bent crystal channeling for $\theta = 0.0°$ (solid black line) are shown in each case, along with two distributions from the volume reflection region (lines and symbols).

oscillations occur for both curvature radii of $R = 50$ μm and 25 μm, though they are more evident for a smaller curvature radius.

In the thicker layer (440 nm) in Figs. 2 and 3(c) the random $\theta_{rms} = 0.10°$ ($\approx\theta_c$). The volume reflected beam is more uniform along the lattice curvature, with a reflected peak around $+0.7\theta_c$. As in thinner layers, the angular width of the reflected peak is only slightly greater than for random incidence, so it is not significantly broadened due to the reflection. Other beam portions are scattered to a range of other exit angles by other factors, such as volume capture which deflects ions to a large negative exit angle.

In the thickest curved layer of 880 nm in Figs. 2 and 3(d) the random $\theta_{rms} = 0.14°$ ($1.4\theta_c$). The volume reflected beam angle and intensity are almost uniform along the lattice curvature, with a reflected peak around $+0.7\theta_c$. In Fig. 2(d) along the lattice curvature from $-0.1°$ to $-0.7°$ the angular width of the reflected peak is similar to that for random incidence, with $\theta_{rms} = 0.16°$. Towards the lower end of the curvature, for tilts of $-0.7°$ to $-1.1°$, the exit distribution widens owing to additional volume capture peaks, separated by θ_c, as shown in Fig. 3(d). Within this tilt range the volume reflected $\theta_{rms} = 0.16°$–$0.18°$, only a small increase compared with random incidence. For a layer thickness of 1760 nm in Fig. 1(a), the random $\theta_{rms} = 0.20°$ ($2\theta_c$), the volume reflected beam is highly uniform along the lattice curvature, and no evidence of any oscillatory behaviour is discernible.

Another previously unreported feature related to volume reflection is shown in Fig. 2(e), where the curved layer is 220 nm thick (random $\theta_{rms} < \theta_c$), and $R = 10$ μm. Here $R < R_c$ so the coherent field of the curved lattice planes is not strong enough to reflect the beam and no bent crystal channeling or volume reflection is expected. Neither is observed in Fig. 2(e) but periodic oscillations in the exit angular distribution are still present along the lattice curvature, with small angular shifts to either side of the incident beam. These occur because the trajectories are still influenced by the curved lattice field when they become tangential to it, even though they are not reflected. They still experience a small deflection on passing through the curved lattice, and the beam is split into two portions resulting in a periodic exit angular distribution as described below. In

thicker layers the periodic oscillations are again obscured by multiple scattering and the exit angular distribution along the lattice curvature is uniform.

Periodic oscillations in the volume reflected angular distributions observed at different tilts in Figs. 2 and 3 are caused by the beam being separated into two portions on passing through the curved lattice. Fig. 4 shows simulated trajectories of 5 MeV protons passing through the same curved lattice at the same two negative tilts shown in Fig. 3(b). In Fig. 4(a), one beam portion enters on the left side of the entrance plane (light-coloured (red online) trajectories) away from the curved lattice. It first encounters the lattice with a low transverse potential energy and is reflected from it. The second beam portion (black trajectories) enters closer to the curved lattice planes and first encounters the lattice with a higher transverse potential energy, so passes through the curved planes. It then encounters the lattice a second time at a greater depth, where the lattice is tilted to a more negative angle. The transverse potential energy of this second beam portion is now not high enough to pass through the curved lattice so it is reflected through an angle different to that of the first beam portion. In Fig. 4(b), the same occurs, but now respectively during the second and third encounters with the lattice since the incident tilt angle is larger, resulting in periodic oscillations along the lattice curvature angle. The amount of beam in each portion determines whether the exit angular distribution is very broad, as for $\theta = -0.22°$, or contains a well-resolved reflected peak, as at $\theta = -0.28°$.

As a rough guide, oscillations are expected in the volume reflected angular distribution along the angular region subtended by the lattice curvature when the random $\theta_{rms} \leqslant \theta_c$. For non-relativistic MeV proton energies the angular scattering of a proton beam energy E through a random layer thickness z is approximately:

$$\theta_r\,(\text{degrees}) \approx 0.75\frac{\sqrt{z\,(\mu\text{m})}}{E\,(\text{MeV})}. \quad (1)$$

The channeling critical angle for a proton energy E along the silicon (1 1 0) planes is

$$\theta_c\,(\text{degrees}) \approx \frac{0.22}{\sqrt{E\,(\text{MeV})}}. \quad (2)$$

Combining (1) and (2) gives a rough upper limit for the layer thickness as

$$z\,(\mu\text{m}) \leqslant 0.088E\,(\text{MeV}). \quad (3)$$

For layer thicknesses below this limit, equal to 440 nm for 5 MeV protons, strong oscillations in the volume reflected beam intensity may be expected. Above this limit, weak oscillations are present, which decrease in intensity for thicker layers. A thickness limit at very high, relativistic GeV proton energies is

$$z\,(\text{mm}) \leqslant 0.18E\,(\text{GeV}). \quad (4)$$

3. Simulated NEP

The effect on the Nuclear Encounter Probability (NEP) of tilting the beam through alignment with the curved lattice is shown in Fig. 5. Fig. 5(a) shows the NEP as a function of incident beam angle for 5 MeV protons for the same layer thicknesses as Fig. 2(a), (c) and (d). The dip in the NEP for beam angles within $\pm\theta_c$ is due to the beam fraction which undergoes bent crystal channeling being less likely to interact with the lattice nuclei. For negative tilts strong oscillations in the NEP are present for $z \leqslant 440$ nm. In thicker layers oscillations reduce in intensity and by $z = 880$ nm the distribution is almost uniform. Fig. 5(b) shows the NEP as a function of incident beam angle for different energy protons. Oscillations are present at beam energies of 5 MeV and above. They occur even when the beam energy exceeds the critical channeling radius, a similar observation to the continued presence volume reflection oscillations in Fig. 2(e). For proton energies of 3 MeV and lower, oscillations have almost disappeared.

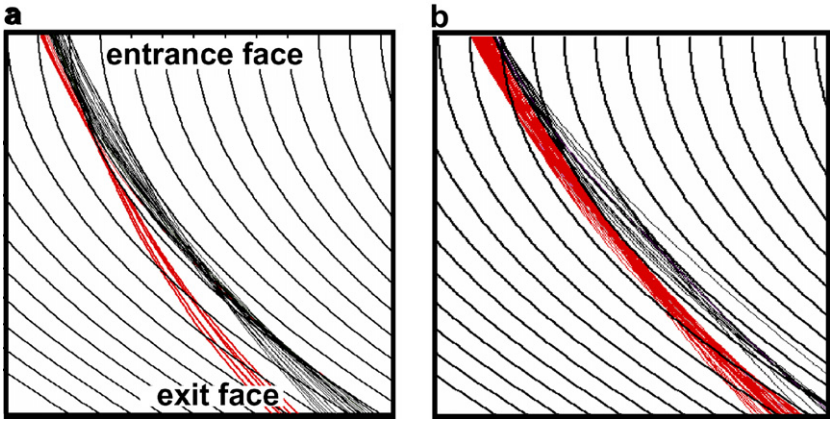

Fig. 4. Simulations of 100 trajectories uniformly distributed across a single (1 1 0) curved lattice plane at the top, entrance surface, for (a) $\theta = -0.22°$, (b) $\theta = -0.28°$, through the curved lattice in Figs. 2 and 3(b). The horizontal × vertical dimensions are 25 nm × 220 nm. The curved planes are shown as thick black lines. The light-coloured (red online) and the black trajectories are those which are reflected from the lattice during different encounters.

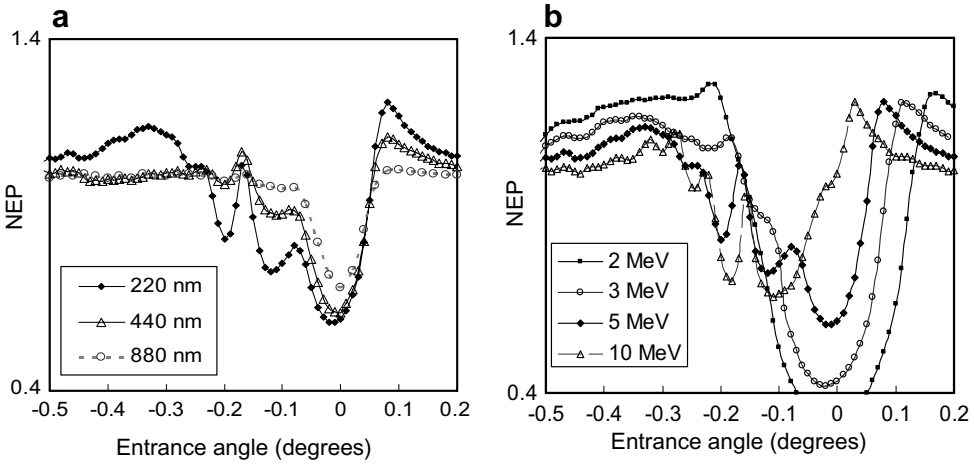

Fig. 5. Simulated NEP for (a) 5 MeV protons along a lattice curvature of $R = 50$ μm with different layer thicknesses, and (b) a fixed layer thickness of $z = 220$ nm with $R = 50$ μm, for different proton beam energies.

The NEP and the volume reflected angular distribution vary in a similar manner with layer thickness; oscillations are present in thin layers where $\theta_{rms} \leqslant \theta_c$, and reduce in intensity in thicker layers where $\theta_{rms} > \theta_c$. It is reasonable to attribute the similarity in behaviour to the same underlying cause described in Fig. 4, whereby the beam which is incident along the lattice curvature is periodically split into several components on passing through successive curved lattice walls, each of having a greater or lesser probability of interacting with the atomic nuclei.

4. Extension to GeV an TeV energies

In a recently-published study [12], volume reflection was simulated for 980 GeV protons incident at tilt angles along the curved (1 1 0) planes of a 5 mm long Si crystal which was bent through $\delta = 440$ μrad. From Eq. (4), the curved crystal length below which they occur is approximately 176 mm for 980 GeV protons. Here $\theta_c = 5.5$ μrad and for randomly incident protons $\theta_{rms} = 3.3$ μrad. Since $\theta_{rms} \leqslant \theta_c$, volume reflection oscillations in the exit angular distributions and in the NEP along the lattice curvature, similar to those observed in Figs. 2 and 5 may be observed if the incident beam divergence is small and it is tilted in sufficiently small angular increments. A volume reflection angle of 4.2 μrad (about $0.7\theta_c$, as in Figs. 2 and 3), with an increased $\theta_{rms} = 6.4$ μrad, was reported in simulations [12], with the behaviour independent of tilt angle along the lattice curvature. The large increase in θ_{rms} along the lattice curvature compared with random incidence supports the prediction that periodic volume reflection is present, since this is associated with periodic oscillations. Similar simulations of the RHIC experiments with 100 GeV/u gold ions ($\theta_c = 11$ μrad, random $\theta_{rms} =$ 12.9 μrad), also gave a uniform volume reflection angle of -15.6 μrad, independent of tilt angle. Here the random $\theta_{rms} > \theta_c$ so only very faint volume reflection oscillations are expected.

5. Experimental results

Direct experimental observation of volume reflection in the transmitted angular distribution at MeV energies is difficult since a curved layer of a few hundred nanometers is too thin to prepare as an adequately flat, free-standing structure and any attached substrate obscures the small volume reflected beam fraction through a large increase in angular scattering. Instead, the same approach as [8,12] is taken whereby the incident beam angle is varied with respect to the curved layer. In this case it is done using a beam-rocking system [17] and the resulting interaction yield is measured as a function of tilt angle. It was shown previously how a curved layer suitable for bending MeV ions can be produced by growing a graded silicon–germanium epitaxial layer on a [0 0 1] Si substrate [18]. The graded $Si_{1-x}Ge_x$ layer has a Ge fraction which varies linearly from zero at the epilayer interface to a maximum at the surface. The resultant tetragonal strain produces a uniformly curved lattice when viewed along off-normal directions and deflection of 2–5 MeV protons was demonstrated [18–20]. Here the epilayer has a Ge fraction varying from $x = 0$ to 0.16, resulting in (1 1 1) planes bent through $\delta = 0.33°$ with $R = 50$ μm in a curved layer thickness of 220 nm.

For this study, the highest available proton beam energy was 3 MeV, for which no strong oscillations are expected in the NEP. Fig. 6 shows the measured yield of Si K_α X-rays produced by tilting a 3 MeV proton beam through alignment with the surface (1 1 1) planes [18,19]. The lattice curvature radius is greater than $R_c = 8$ μm so beam which is incident within $\pm\theta_c$ is deflected, producing a dip in the measured yield. To the right the yield rises to the random value at about $+\theta_c$. To the left is a region where the yield is between the random and channeled values, extending from about $-\theta_c$ to $-(\theta_c + \delta)$. The behaviour is similar to that observed at GeV energies in a multi-turn geometry [8,12], though here it is observed at MeV energies in a single-pass mode and the region of reduced yield extends by θ_c

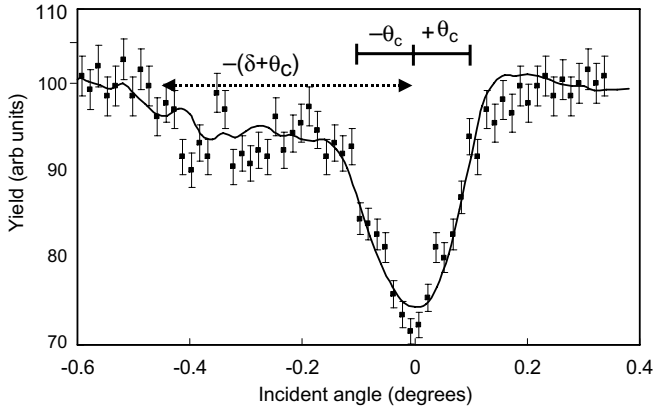

Fig. 6. Measured X-ray yield versus incident tilt angle θ across the entrance (1 1 1) planes of a graded $Si_{1-x}Ge_x$ epilayer when aligned close to the [1 1 2] axis. The beam current of 3 MeV protons was 200 pA, and X-rays were recorded using a 80 mm^2 Si(Li) detector. The error bars are determined solely by the X-ray counting statistics. The solid line shows the simulated NEP, including the attached substrate.

beyond the lattice curvature. The NEP is not directly comparable to the X-ray yield since X-rays originate from inner-shell electrons rather than atomic scattering, and X-rays are recorded from the silicon substrate as well as the curved epilayer. However, reasonable agreement is obtained with the location and extent of the region of reduced yield, and the absence of oscillations in the NEP at such a low energy.

6. Conclusions

In conclusion, the conditions under which oscillations in the volume reflected angular distribution and in the NEP occur have been determined. They are present when the curved layer is thin enough such that the multiple scattering angle at random incidence is less than the channeling critical angle. In thicker curved layers, oscillations disappear since the behaviour is dominated by multiple scattering. The same origin of oscillations observed in simulations of volume reflection and NEP is attributed. Oscillations were not resolved in experiments at such low proton energies, in agreement with simulations, but are predicted to occur at higher energies or in thinner layers. This may provide a way of deducing the cause of the reduced yield along the lattice curvature as either volume reflection or volume capture.

References

[1] E. Tsyganov, Fermilab TM-682, TM-684, Batavia, 1976, unpublished.
[2] V.M. Biryukov, Yu.A. Chesnokov, V.I. Kotov, Crystal Channeling and its Application at High Energy Accelerators, Springer, Berlin, 1997.
[3] V.M. Biryukov, Phys. Rev. Lett. 74 (1995) 2471.
[4] X. Altuna et al., Phys. Lett. B 357 (1995) 671.
[5] A.G. Afonin, V.T. Baranov, V.M. Biryukov, V.N. Chepegin, Yu.A. Chesnokov, Yu.S. Fedotov, A.A. Kardash, V.I. Kotov, V.A. Maisheev, V.I. Terekhov, E.F. Troyanov, Nucl. Instr. and Meth. B 234 (2005) 14.
[6] H. Akbari et al., Phys. Lett. B 313 (1993) 491.
[7] A.G. Afonin et al., Phys. Lett. B 435 (1998) 240.
[8] R.P. Fliller, A. Drees, D. Gassner, L. Hammons, G. McIntyre, S. Peggs, D. Trbojevic, V.M. Biryukov, Y. Chesnokov, V. Terekhov, Phys. Rev. ST AB 9 (2006) 013501.
[9] A.G. Afonin et al., Phys. Rev. Lett. 87 (2001) 094802.
[10] V.A. Andreev et al., JETP Lett. 36 (1982) 415.
[11] A.M. Taratin, A.A. Vorobiev, Phys. Lett. A 119 (1987) 425.
[12] V.M. Biryukov, in: EPAC Proc. (Edinburgh, 2006) pp. 945–949 and e-print arxiv:physics/0602012.
[13] P.J.M. Smulders, D.O. Boerma, M. Shaanan, Nucl. Instr. and Meth. B 45 (1990) 450.
[14] P.J.M. Smulders, D.O. Boerma, Nucl. Instr. and Meth. B 29 (1987) 471.
[15] J.F. Ziegler, J.P. Biersack, U. Littmark, in: The Stopping and Range of Ions in Solids, Pergamon Press, New York, 1985, p. 41.
[16] J. Lindhard, K. Dan, Viddensk. Selsk. Mat. Phys. Medd. 34 (1) (1965).
[17] D.G. de Kerckhove, M.B.H. Breese, G.W. Grime, Nucl. Instr. and Meth. B 129 (1997) 534.
[18] M.B.H. Breese, Nucl. Instr. and Meth. B 132 (1997) 540.
[19] D.G. de Kerckhove, M.B.H. Breese, P.J.M. Smulders, D.N. Jamieson, Appl. Phys. Lett. 74 (1999) 227.
[20] M.B.H. Breese, D.G. de Kerckhove, P.J.M. Smulders, W.M. Arnold Bik, D.O. Boerma, Nucl. Instr. and Meth. B 171 (2000) 387.